Temporally resolved imaging on quenching and re-ignition of nanosecond underwater discharge

Yong Yang, Young I. Cho and Alexander Fridman
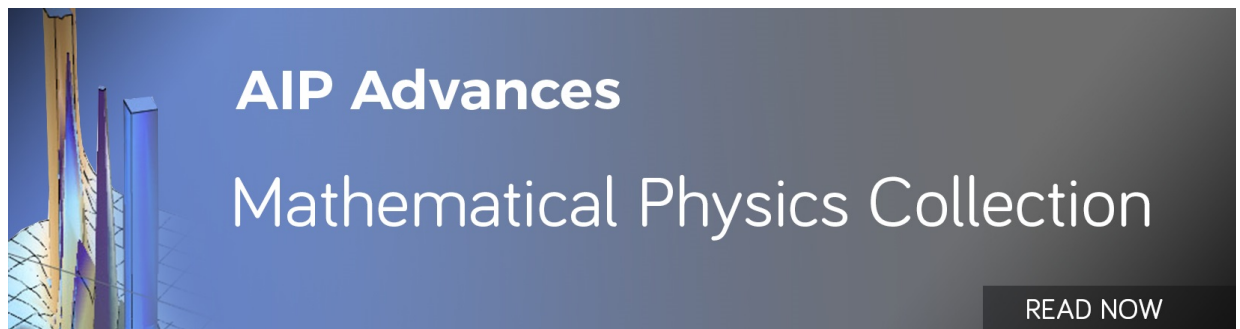
View Online   Export Citation   CrossMark

ARTICLES YOU MAY BE INTERESTED IN

Retraction: "Temporally resolved imaging on quenching and re-ignition of nanosecond underwater discharge" [AIP Advances 2, 042153 (2012)]
AIP Advances **3**, 079901 (2013); https://doi.org/10.1063/1.4813235

Underwater streamer propagation analyzed from detailed measurements of pressure release
Journal of Applied Physics **101**, 053302 (2007); https://doi.org/10.1063/1.2437675

Initiation process and propagation mechanism of positive streamer discharge in water
Journal of Applied Physics **116**, 213301 (2014); https://doi.org/10.1063/1.4902862

AIP Advances

Mathematical Physics Collection

READ NOW

2, 042153

Temporally resolved imaging on quenching and re-ignition of nanosecond underwater discharge

Yong Yang,[1,a] Young I. Cho,[2] and Alexander Fridman[2]
[1]*State Key Laboratory of Advanced Electromagnetic Engineering and Technology, Huazhong University of Science and Technology, Wuhan, Hubei 430074, China*
[2]*Department of Mechanical Engineering, Drexel University, Philadelphia, PA 19104, USA*

This paper presents the temporally resolved images of plasma discharge in de-ionized water. The discharge was produced by high voltage pulses with 0.3 ns rise time and 10 ns duration. The temporal resolution of the imaging system was one nanosecond. A unique three-stage process, including a fast ignition at the leading edge of the pulse, quenching at the plateau of the pulse, and self re-ignition at the trailing edge of the pulse, was observed in a single pulse cycle. The maximum measured propagation velocity of the plasma discharge was about 1000 km/s. The possibility of direct ionization in water under high reduced electric field conditions was discussed. *Copyright 2012 Author(s). This article is distributed under a Creative Commons Attribution 3.0 Unported License*. [http://dx.doi.org/10.1063/1.4769080]

I. INTRODUCTION

Over the past few decades, different types of underwater plasma discharge have been extensively studied. An overview of earlier research was given by Locke *et al.*[1] More recently, Bruggeman and Leys[2] published an excellent review on the current state of the art of underwater plasma generation. Current interest in plasma discharge in water is mainly driven by its potential application in biological, environmental and nanoscience areas.[3] One of the major advantages of underwater plasma discharge is that it combines different effects, including radical species (OH, O, HO_2, *etc.*), molecular species (H_2O_2, O_3, *etc.*), ultraviolet (UV) radiation, electric field and shockwaves, in a single process. The synergy between these effects is believed to makes them particularly suitable for decontamination and sterilization purposes, and provides a higher efficiency than traditional chemical treatment methods. Secondly, the in-situ production of active chemical species eliminates the need of transportation, storage, and residual remediation of external chemical sources.

Despite the fact that underwater discharge has a long history of study, the mechanism of discharge initiation and propagation is still in dispute. Two complete different explanations to the underwater breakdown mechanism exist from the beginning of related research.[4] The first hypothesis assumes that the breakdown initiates in gas cavities, either already present in the liquid or newly created through joule heating, electrolysis, or other cavitation pathways. This hypothesis is conventionally called the bubble theory. The second hypothesis argues that a gaseous phase is not necessary and direct impact ionization in water is enough to generate the avalanche multiplication of charges, which will eventually lead to the breakdown as in gas-phase discharges. The competition between the bubble theory and the so-called "direct ionization theory" is not conclusive, and the dispute will probably continue on in the near future.

For microsecond or sub-microsecond (with duration time ranging from a few hundred nanoseconds to tens of microseconds) discharges in water, a well observed phenomena is that the propagation of the discharge filaments can be divided into two phases.[5–7] For example, An *et al.*[7] demonstrated that with 40-ns rise time and 10-μs duration time, the development velocity of the discharge is

---

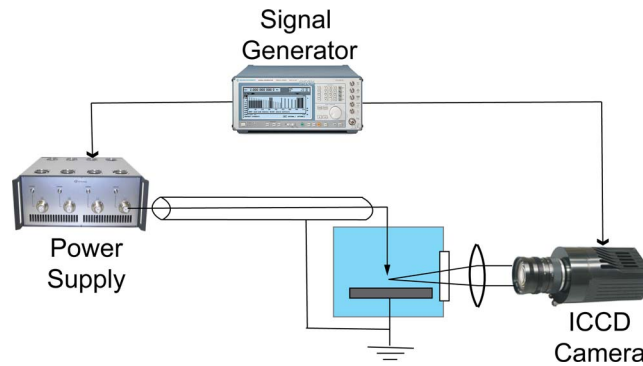[a]Author to whom correspondence should be addressed. Electronic mail: yangyong@hust.edu.cn

FIG. 1. Schematic diagram of experimental setup.

about 2.5 km/s during the primary phase and can reach up to 35 km/s during the secondary phase. Both the shadowgraph and Schlieren images suggested that the filaments were of gaseous nature. A natural question one would raise is: what would happen if the duration of the high voltage pulse is sufficiently short to suppress the hydrodynamic growth of the gaseous plasma filaments? In that case, would the initiation and propagation of the discharge be different for the short pulses?

To answer these questions, a nanosecond pulsed power system (with pulse duration about 10 ns) synchronized with a picosecond ICCD camera (with minimum gate time 50 ps) was used to study the time-resolved evolution of nanosecond discharge in water. The purpose of this paper is to give an experimental insight into the initiation and propagation mechanisms of the plasma filaments through the water under short pulse excitations.

II. EXPERIMENT SETUP

The schematic diagram of the system is shown in Figure 1. A point-to-plane electrode configuration was used. The high-voltage needle electrode had a diameter of 100 μm with radius of curvature at the tip of about 10 μm. The diameter of the ground plane electrode was 18 mm. The inter-electrode distance was 4 mm. Distilled and de-gassed water was used for all experiments (pH about 6.4, conductivity about 5 μS/cm). To initiate the discharge in liquid water, a nanosecond pulsed power system was used. The power supply was made by FID Tech on the basis of solid state switches. It generates pulses with +16 kV pulse amplitude in 50-Ohm coaxial cable (32 kV on the high voltage electrode tip because of pulse reflection), 10 ns pulse duration (90% amplitude), 0.3 ns rise time and 3 ns fall time. The maximum pulse frequency was 5 kHz. The voltage was measured using low-inductive back-current shunts, and the waveform is shown in Figure 2. Current measurement was also attempted by subtracting the displacement current from the total current. However, the displacement current was orders of magnitude higher than the electron/ion current due to the extremely fast rise time (0.3 ns), and it was difficult to separate the contribution of the electron/ion and displacement current from the total discharge current. The time-resolved imaging was performed with the help of 4Picos ICCD camera made by Stanford Computer Optics. The camera has a spectral response from 180 nm to 750 nm. The effective spectral response was 250 nm to 750 nm if taking into account the UV absorption in water. Quartz lens with a focal distance of 70 mm and diameter of 50 mm was used to focus the discharge gap to the photocathode with four-time magnification. Typical camera's field of view was 2.6 × 1.7 mm. The synchronization system for the experiments was built on the basis of Tektronix AFG-3252 Arbitrary/Function Generator. The generator has synchro-output and two adjustable channels with a signal rise/fall time less than 2.5 ns and a typical jitter (RMS) less than 20 ps with a delay time resolution of 10 ps. The generator provides a stable synchronization between high-voltage pulse and camera intensifier.

The pulse frequency in all experiments was fixed at 1 Hz to avoid possible interference from previous discharge. The discharge showed good reproducibility. The optical system used in this work allowed us to catch strong density perturbations (if any) of a size larger than 2 μm. To capture
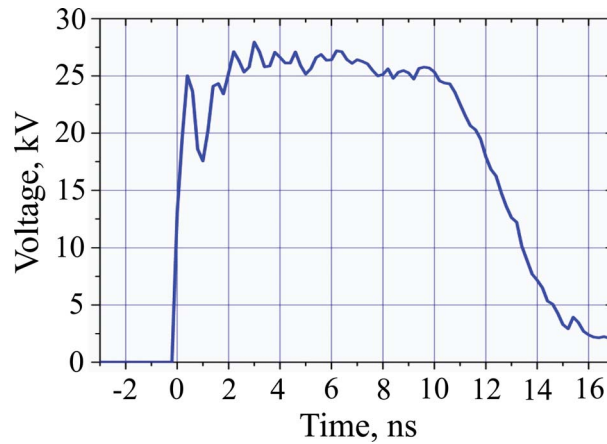
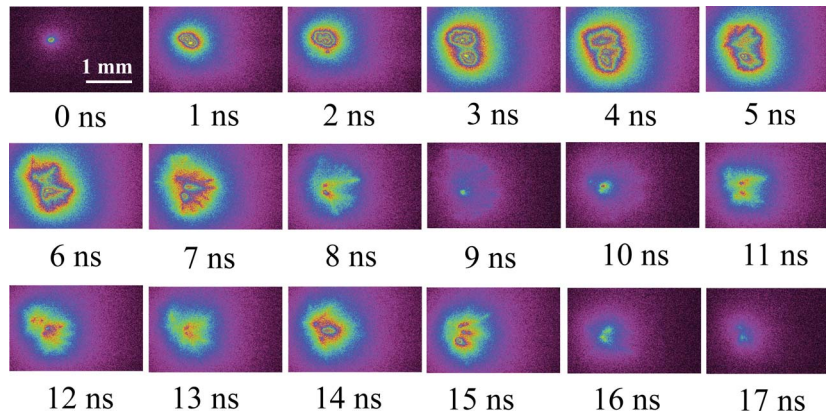FIG. 2. High voltage pulse used in the experiment.

FIG. 3. Temporal-resolved images of nanosecond discharge in water. The camera gate is 1 ns.

the temporal evolution of the discharge, we used a 1-ns camera gate. A sequence of images was obtained using a pulse-by-pulse technique. For each high-voltage pulse, the delay of the intensifier was shifted by 1 ns. r. Optical emission spectra of the discharge were taken in the range 200–900 nm, averaging emission from the entire discharge.

III. RESULTS AND DISCUSSIONS

Figure 3 shows the sequence of images starting from the rise of the high voltage. The color indicates the intensity of light emission received at the ICCD sensor, with red being the strongest emission spot and black being the weakest. From the figure, it is clear that the evolution of the discharge can be subdivided into three stages. At the first stage, the discharge started from the point electrode and propagated in water towards the ground electrode. A maximum velocity of about 1000 km/s (1 mm/ns) was observed during the initial stage. Then, the velocity became lower (about 0.3 mm/ns) after the voltage reached maximum, and finally stopped growing at about t = 6-7 ns. The maximum size of the discharge was about 1.5 mm. After that, the "dark phase" appears, as shown in t = 8-11 ns in Figure 3, with no sufficient discharge emission observed. During this phase the discharge cannot propagate, possibly because of space charge formation and decrease of the electric field. Thus, when the voltage on the electrode started to fall, the electrode potential becomes smaller than the potential of the previously charged region. This led to the re-ignition of the second flash, which corresponds to the charge removal process. The emission from the re-ignition process is slightly weaker than the excitation caused by the leading edge of the pulse. Figure 4 shows the
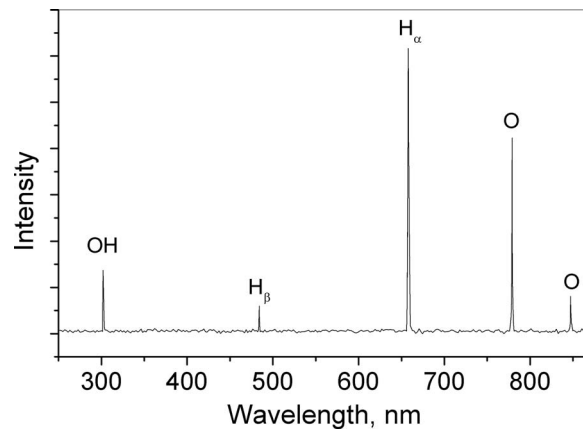
FIG. 4. Time-integrated optical emission spectra of the nanosecond discharge in de-ionized water.

time-integrated optical emission spectra from the discharge. The spectra indicated strong atomic line emissions due to the presence of hydrogen and oxygen radicals from the decomposition of water molecules.

The discharge observed here is different from the discharge produced by microsecond or sub-microsecond duration pulses from aforementioned publications.[5–7] In our case, the discharge demonstrated a more spherical shape with a few major branches, while the microsecond or sub-microsecond discharges usually have a complicated bush-like structure. The propagation of the nanosecond discharge reached about 1000 km/s, which was two orders of magnitude higher than the velocity observed in low density plasma filaments. This velocity is comparable to the velocity of ionization wave in gas phase. Also it should be noted that no bubble formation with size above the system's spatial resolution was observed in our experiments, even after hours of operation at a frequency of 1 Hz. This suggests that the breakdown cannot be explained by the bubble theory.

As mentioned in previous section, another possible mechanism of underwater breakdown is the direct impact ionization by electrons present in the liquid system, which is similar to the breakdown in gas phase. However, the major obstacle for the direct impact ionization hypothesis is that in liquid water, free electrons are rapidly quenched through the attachment process to water molecules. So it would be difficult to maintain a sufficient amount of free electrons in bulk water to initiate the avalanche.

Next we will try to get some insight into the possibility of direct ionization in water under current experimental conditions by comparing the rate coefficient of excitation, ionization and attachment processes. Unfortunately there is no adequate model for non-equilibrium discharge development in dense media. Here we use the "dense gas" approach[8,9] to estimate the electric field needed for water ionization. The "dense gas" approach assumes that the liquid is a gas but with high particle number density. This approximation neglects the multi-particle interaction in liquid phase and uses electron-molecule interaction cross-sections obtained in gas phase for liquid phase interactions. This simplification could lead to significant deviations from the real situation. However, the approach does provide at least qualitative estimations for the process.

We used cross-section and threshold energy data from Hayashi[10] and Gianturco *et al.*[11] to analyze the ratio among the rate of electron's excitation, attachment and ionization (Figure 5). Figure 6 shows the rate coefficients for different processes as functions of reduced electric field E/n (ratio of the electric field strength to the particle number density) in room temperature water vapor calculated using method described by Hagelaar and Pitchford.[12] Again, it should be noted that these data cannot give quantitative description of the processes in liquid water and we will use them for evaluation purposes only. From Figure 5 it is clear that the ionization rate becomes higher than the attachments for $E/n > 50$ Td. At $E/n = 100$ Td, the rate coefficient for ionization is already one order of magnitude higher than those for attachments processes. In real condense media, multi-body attachments will play the major role. Taking into account a strong dependence of the rate constant of
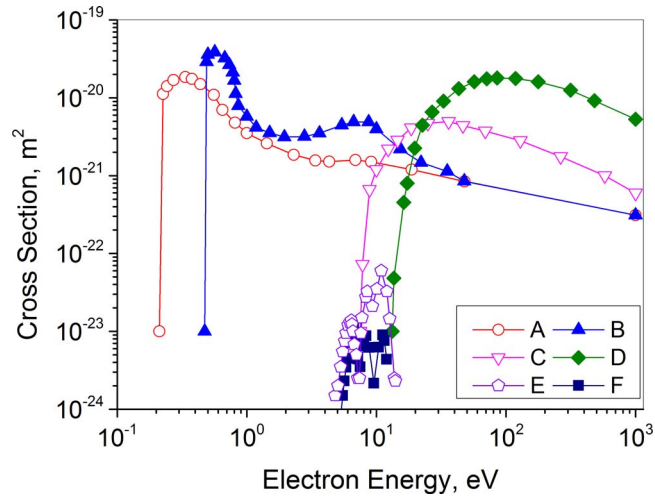
FIG. 5. Cross-sections (in [m^2]) for H$_2$O vapor. A: vibrational excitation (0.20 eV); B: vibrational excitation (0.45 eV); C: electronic excitation (7.10 eV); D: ionization (12.61 eV); E: dissociative attachment (e + H$_2$O → OH$^-$ + H, 3.28 eV); F: dissociative attachment (e + H$_2$O → H$_2$ + O$^-$, 3.58 eV).
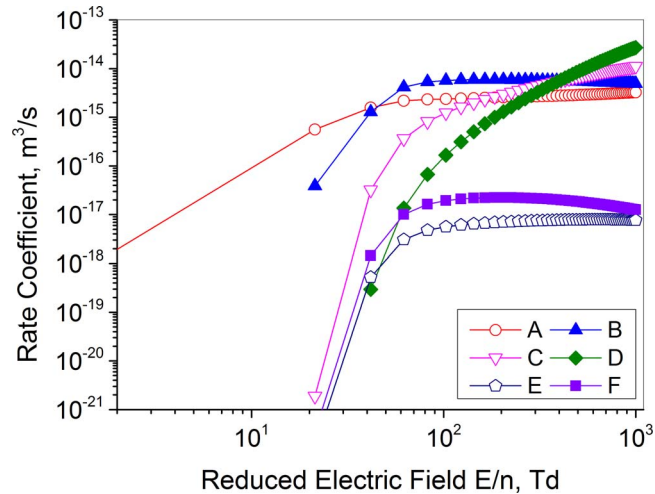

FIG. 6. Rate coefficients for different processes in water vapor in dependence on the E/n value. A: vibrational excitation (0.20 eV); B: vibrational excitation (0.45 eV); C: electronic excitation (7.10 eV); D: ionization (12.61 eV); E: dissociative attachment (e + H$_2$O → OH$^-$ + H, 3.28 eV); F: dissociative attachment (e + H$_2$O → H$_2$ + O$^-$, 3.58 eV).

ionization from E/n we can assume, nevertheless, that for E/n > 100 Td we can obtain fast ionization even in the condensed media. At normal conditions it means that the electric field value should be close or greater than E$_{crit}$ > 30 MV/cm. Given the geometrical parameters of the electrode with radius of curvature at the tip of about 10 μm, we can estimate the electric field in our experiments to be E ∼ 27 MV/cm (E/n ∼ 82 Td), which is close to the critical electric field estimated using dense-gas model. Thus we can assume that the direct ionization by electron impact is possible in liquid water at the initial stage. As the size of the discharge grows, the electric field becomes weaker at the ionization front. This may explain why the discharge stops growing and finally enters the dark phase, when the electric field is not high enough to sustain the ionization process. At the trailing edge of the pulse, the electric field from the electrode drops. But the electric field induced by the space charges remains, and may be responsible for the re-ignition of the second flash.

IV. CONCLUSIONS

In summary, here we presented the time-resolved imaging of nanosecond discharge in water. The duration of the high voltage pulse was about 10 ns, and the time resolution of the imaging system was 1 ns. A unique three-stage process was observed, which involved quenching and re-ignition of the discharge in a single pulse cycle. Propagation velocity up to 1000 km/s was recorded, which was two orders of magnitude higher than that obtained in experiments with microsecond duration times. The results suggest different mechanism of initiation, and the estimation using the "dense gas" approximation shows that the observed phenomena may be explained by direct impact ionization process.

ACKNOWLEDGMENT

[1] B. R. Locke, M. Sato, P. Sunka, M. R. Hoffmann, and J. S. Chang, Ind. Eng. Chem. Res. **45**, 882 (2006).
[2] P. Bruggeman and C. Leys, J. Phys. D: Appl. Phys. **42**, 053001 (2009).
[3] W. G. Graham and K. R. Stalder, J. Phys. D: Appl. Phys. **44**, 174037 (2011).
[4] J. Kolb, R. Joshi, S. Xiao, and K. Schoenbach, J. Phys. D: Appl. Phys. **41**, 234007 (2008).
[5] H. Akiyama, IEEE Trans. Dielectr. Electr. Insul. **7**, 646 (2000).
[6] P. H. Ceccato, O. Guaitella, M. Rabec Le Gloahec, and A. Rousseau, J. Phys. D: Appl. Phys. **43**, 175202 (2010).
[7] W. An, K. Baumung, and H. Bluhm, J. Appl. Phys. **101**, 053302 (2007).
[8] V. M. Atrazhev, E. G. Dmitriev, and I. T. Iakubov, IEEE Trans. Electr. Insul. **26**, 586 (1991).
[9] V. M. Atrazhev and I. V. Timoshkin, IEEE Trans. Dielectr. Electr. Insul. **5**, 450 (1998).
[10] M. Hayashi, *Swarm Studies and Inelastic Electron-Molecule Collision.* (Springer-Verlag, New York, 1987), p.167.
[11] F. A. Gianturco and D. G. Thompson, J. Phys. B: At. Mol. Phys. **13**, 613 (1980).
[12] G. J. M. Hagelaar and L. C. Pitchford, Plasma Sources Sci. Technol. **14**, 722 (2005).